

## Nanopattern Formation from Tethered PS-*b*-PMMA Brushes upon Treatment with Selective Solvents

Bin Zhao, William J. Brittain,\* Wensheng Zhou, and Stephen Z. D. Cheng

Department of Polymer Science  
The University of Akron, Akron, Ohio 44325-3909

Received July 13, 1999

Patterned organic films are important in microelectronics,<sup>1</sup> cell growth control,<sup>2,3</sup> and biomimetic materials fabrication.<sup>4</sup> The preparation of micro-patterned polymer films has been achieved by photolithographic techniques.<sup>1</sup> Microcontact printing, a method for patterning self-assembled monolayers has been reported,<sup>5</sup> and has been extended into patterning polymer films.<sup>6–11</sup> Another route for designing patterned polymer films, which has been discussed theoretically but has not been experimentally confirmed, is fabrication of tethered block copolymer films and treatment with selective solvents.<sup>12–15</sup>

The phase behavior of bulk block copolymers has been extensively studied.<sup>16,17</sup> For diblock copolymers with immiscible components, microphase separation occurs. Under a strong segregation limit, linear diblock copolymers in the bulk exhibit ordered morphologies that depend on the volume composition. When the diblock copolymer is near a surface or confined between two solid surfaces, it self-assembles into an ordered structure with a specific microdomain orientation, either parallel or normal to the surface, depending on the interaction between the blocks in the copolymers and interfaces.<sup>18–22</sup>

The phase behavior of diblock copolymer brushes that are tethered to a planar surface is interesting. Like bulk systems, the Flory–Huggins interaction parameter ( $\chi$ ), molecular weight ( $N$ ) and volume fraction of diblock copolymer ( $f$ ) are important. Other factors, such as covalent attachment of diblock copolymer chain ends, environmental conditions (solvent, temperature), and surface free energy of each block in air are also critical in determining

phase morphologies. Using 2-dimensional self-consistent field (SCF) calculations and scaling arguments,<sup>12–15</sup> it has been predicted that novel structures for tethered diblock copolymer brushes should be formed. By controlling the chain architecture, grafting density, molecular lengths of the copolymer and its individual components, interaction energy between different blocks, and interaction energies between blocks and solvents one can design patterned polymer films by forming a series of well-defined structures such as “onion”, “garlic”, “dumbbell”, flowerlike, checkerboard, and others. While there has been extensive theoretical and experimental research on homopolymer brushes,<sup>23</sup> no experimental results have been reported on tethered diblock copolymer brushes.

In this contribution, we report the X-ray photoelectron spectroscopy (XPS) and atomic force microscopy (AFM) studies of tethered polystyrene-*b*-poly(methyl methacrylate) (PS-*b*-PMMA).<sup>24</sup> The copolymer brushes have been characterized by using tapping mode AFM. The synthesis of tethered PS-*b*-PMMA on silicate substrates was accomplished by a sequential process involving carbocationic polymerization of styrene followed by atom transfer radical polymerization of methyl methacrylate (MMA).<sup>25–27</sup> As described in earlier publications, the advancing water contact angle of tethered PS-*b*-PMMA brushes increases from 74° (characteristic value for PMMA) to 99° (characteristic value for PS) when the sample is treated with methylcyclohexane or cyclohexane, which are better solvents for PS than for PMMA. This contact-angle change is reversible. Treatment of the sample with CH<sub>2</sub>Cl<sub>2</sub>, which is a good solvent for both PS and PMMA, changes the advancing contact angle back to 74°. Since the initiation efficiency of surface-initiated cationic polymerization is low,<sup>25–27</sup> the tethered diblock copolymer chains may have enough three-dimensional space to reorganize. The XPS results of a tethered PS-*b*-PMMA with 28 nm thick PS layer and 11 nm thick PMMA layer<sup>28</sup> treated with CH<sub>2</sub>Cl<sub>2</sub> and cyclohexane indicate large compositional changes on the topmost layer, which is consistent with the contact angle observations. The sampling depth of XPS experiments is ~5–10 nm depending on the core level binding energy and takeoff angle.<sup>29</sup> The O<sub>1s</sub> peak intensity decreases significantly after cyclohexane treatment.<sup>33</sup> The molar

(1) Niu, Q. J.; Fréchet, J. M. J. *Angew. Chem., Int. Ed.* **1998**, *37*, 667–670.

(2) Singhvi, R.; Kumar, A.; Lopez, G. P.; Stephanopoulos, G. N.; Wang, D. I. C.; Whitesides, G. M.; Ingber, D. E. *Science* **1994**, *264*, 696–698.

(3) Chen, C. S.; Mrksich, M.; Huang, S.; Whitesides, G. M.; Ingber, D. E. *Science* **1997**, *276*, 1425–1428.

(4) Aksay, A.; Trau, M.; Manne, S.; Honma, I.; Yao, N.; Zhou, L.; Fenter, P.; Eisenberger, P. M.; Gruner, S. M. *Science* **1996**, *273*, 892–898.

(5) Xia, Y.; Whitesides, G. M. *Angew. Chem., Int. Ed.* **1998**, *37*, 550–575.

(6) Husemann, M.; Mecerreyes, D.; Hawker, C. J.; Hedrick, J. L.; Shah, R.; Abott, N. L. *Angew. Chem., Int. Ed.* **1999**, *38*, 647–649.

(7) Lackowski, W. M.; Ghosh, P.; Crooks, R. M. *J. Am. Chem. Soc.* **1999**, *121*, 1419–1420.

(8) Ghosh, P.; Amirpour, M. L.; Lackowski, W. M.; Pishko, M. V.; Crooks, R. M. *Angew. Chem., Int. Ed.* **1999**, *38*, 1592–1595.

(9) Böltau, M.; Walheim, S.; Mlynek, J.; Krausch, G.; Steiner, U. *Nature* **1998**, *391*, 877–879.

(10) Karim, A.; Douglas, J. F.; Lee, B. P.; Glotzer, S. C.; Rogers, J. A.; Jackman, R. J.; Amis, E. J.; Whitesides, G. M. *Phys. Rev. E* **1998**, *57*, R6273–6276.

(11) Hammond, P. T.; Whitesides, G. M. *Macromolecules* **1995**, *28*, 7569–7571.

(12) Zhulina, E. B.; Singh, C.; Balazs, A. C. *Macromolecules* **1996**, *29*, 6338–6348.

(13) Singh, C.; Balazs, A. C. *Macromolecules* **1996**, *29*, 8904–8911.

(14) Zhulina, E.; Singh, C.; Balazs, A. C. *Macromolecules* **1996**, *29*, 8254–8259.

(15) Zhulina, E.; Balazs, A. C. *Macromolecules* **1996**, *29*, 2667–2673.

(16) Bates, F. S. *Science* **1991**, *251*, 898–905.

(17) Bates, F. S.; Fredrickson, G. H. *Annu. Rev. Phys. Chem.* **1990**, *41*, 525–557.

(18) Russell, T. P. *Curr. Opin. Colloid Interface Sci.* **1996**, *1*, 107–115.

(19) Huang, E.; Rockford, L.; Russell, T. P.; Hawker, C. J. *Nature* **1998**, *395*, 757–758.

(20) Mansky, P.; Russell, T. P.; Hawker, C. J.; Pitsikalis, M.; Mays, J. *Macromolecules* **1997**, *30*, 6810–6813.

(21) Lambooy, P.; Russell, T. P.; Kellogg, G. J.; Mayes, A. M.; Gallagher, P. D.; Satija, S. K. *Phys. Rev. Lett.* **1994**, *72*, 2899–2902.

(22) Koneripalli, N.; Singh, N.; Levicky, R.; Bates, F. S.; Gallagher, P. D.; Satija, S. K. *Macromolecules* **1995**, *28*, 2897–2904.

(23) Recent examples include: (a) Husseman, M.; Malmstrom, E. E.; McNamara, M.; Mate, M.; Mecerreyes, O.; Benoit, D. G.; Hedrick, J. L.; Mansky, P.; Huang, E.; Russell, T. P.; Hawker, C. J. *Macromolecules* **1999**, *32*, 1424–1431. (b) Weck, M.; Jackiw, J. J.; Rossi, R. R.; Weiss, P. S.; Grubbs, R. H. *J. Am. Chem. Soc.* **1999**, *121*, 4088–4089. (c) Huber, D. L.; Gonsalves, K. E.; Carlson, G.; Seery, T. A. P. In *Interfacial Aspects of Multicomponent Polymer Materials*; Lohse, D. J., Russell, T. P., Sperling, L. H., Eds.; Plenum Press: New York, 1997; pp 107–122.

(24) AFM images were obtained using a Multimode Scanning Probe Microscopy (Digital Instruments) in tapping mode with a silicon tip. XPS was performed on a Perkin-Elmer instrument using Al K $\alpha$  radiation at the MATNET Surface Analysis Center at Case Western Reserve University. The incidence angle of X-rays was 45° with respect to surface normal. Survey spectra were taken after the sample was treated with CH<sub>2</sub>Cl<sub>2</sub> and cyclohexane.

(25) Zhao, B.; Brittain, W. J. *J. Am. Chem. Soc.* **1999**, *121*, 3557–3558.

(26) Zhao, B.; Brittain, W. J. *Macromolecules* **2000**, *33*, 342–348.

(27) Zhao, B.; Brittain, W. J. *Polym. Prepr. (Am. Chem. Soc. Div. Polym. Chem.)* **1999**, *40*(2), 159–160.

(28) The thicknesses of tethered PS and diblock copolymer films were obtained using a Gaertner model L116C ellipsometer; the refractive index of polymer film was fixed at 1.500 after CH<sub>2</sub>Cl<sub>2</sub> treatment or THF extraction.

(29) Briggs, D. In *Surface Analysis of Polymers by XPS and Static SIMS*; Clarke, D. R., Suresh, S., Ward FRS, I. M., Eds., Cambridge University Press: Cambridge, 1998.

(30) Mansky, P.; Liu, Y.; Huang, E.; Russell, T. P.; Hawker, C. J. *Science* **1997**, *275*, 1458–1460.

(31) Experimental procedure for sample treatment: the sample was immersed in CHCl<sub>3</sub> or CH<sub>2</sub>Cl<sub>2</sub> at 35 °C for 30 min. 50% of the solvent volume was replaced with an equal volume of cyclohexane. The sample was treated in each solvent composition for 30 min at 35 °C. This procedure was repeated until cyclohexane: CH<sub>2</sub>Cl<sub>2</sub> (CHCl<sub>3</sub>) > 99.5:0.5 (v/v). After the sample was taken out of the solvent and dried by a clean air stream, it was subjected to AFM study.

(32) Ulman, A. *An Introduction to Ultrathin Organic Films*; Academic Press: Boston, 1991.

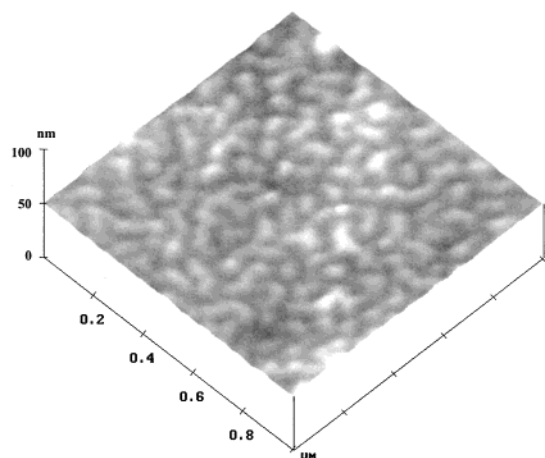


**Figure 1.** AFM image of the tethered PS-*b*-PMMA brushes with 23 nm thick PS layer and 14 nm thick PMMA layer after treatment with CH<sub>2</sub>Cl<sub>2</sub> at room temperature for 30 min and drying with a clean air stream.

contents of C and O atoms are 76.5 and 23.5%, respectively, after treatment with CH<sub>2</sub>Cl<sub>2</sub>; treatment with cyclohexane decreases the oxygen content to 7.8%. Although X-rays can damage the sample by decomposing PMMA units,<sup>29</sup> the XPS results on different sample locations are similar (variations of C and O contents <1.5%). Therefore, we conclude that the XPS results provide reliable information.

Tensiometry and XPS are surface macroscopic characterization techniques. We utilized AFM to examine microscopic morphology. Figures 1–3 are AFM images of tethered PS-*b*-PMMA brushes with 23 nm thick PS layer and 14 nm thick PMMA. Figure 1 is the AFM image after the sample was immersed in CH<sub>2</sub>Cl<sub>2</sub> at room temperature for 30 min and then dried under a flow of clean air. The surface is relatively smooth; the roughness is 0.77 nm, where roughness is defined as root-mean-square of height deviations taken from the mean data plane. Since CH<sub>2</sub>Cl<sub>2</sub> is a good solvent for both PS and PMMA blocks, the tethered PS-*b*-PMMA chains possess extended conformations. The PMMA-blocks cover the topmost layer and exhibit an advancing water contact angle of 74°. Note that surface free energies of PS and PMMA in air are very close to each other,<sup>30</sup> and removing the sample from the solvent and drying the copolymer brushes should not significantly change the original arrangement of molecular conformations except for further microphase segregation of the PMMA- and PS-blocks.

After cyclohexane treatment at 35 °C for 1 h and drying under air, the advancing contact angle increases to 99°. In Figure 2, the AFM result shows that the film surface becomes relatively rough with a roughness of 1.79 nm. Irregular wormlike networks appear on the film. At 35 °C, cyclohexane is a  $\theta$  solvent for the PS-blocks and a poor solvent for the PMMA-blocks. The PS-blocks are swollen with cyclohexane while the PMMA-blocks are collapsed. Both effects lead to opposite movement of the blocks and hence, networks are formed.

If mixed solvents of CH<sub>2</sub>Cl<sub>2</sub> and cyclohexane are used and % cyclohexane is gradually increased,<sup>31</sup> the tethered diblock chains reorganize. With increasing cyclohexane content, the PMMA-blocks collapse and aggregate to form a core. For the PS-blocks, both ends are connected covalently; one is tethered on the surface, and the other end is connected to the PMMA-block. Consequently, their mobility is highly restricted, and we speculate that the PS-blocks form a layer around the PMMA core, resulting in an array of micelles with an ellipsoidal shape as shown in Figure 3. The roughness in this surface is as high as 13.08 nm, and the half-height ellipsoid size is relatively uniform at 85 nm. The ellipsoid height is 55 nm although the initial brush thickness is only 37 nm. The advancing water contact angle is 120°, which is 21° higher than the characteristic value of PS. Surface roughness

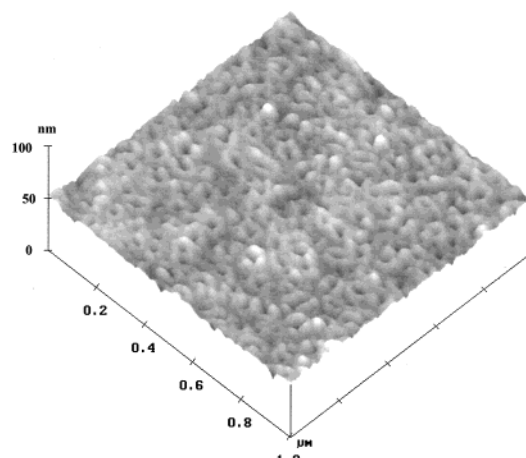


**Figure 2.** AFM image of the tethered PS-*b*-PMMA brushes with 23 nm thick PS layer and 14 nm thick PMMA layer after treatment with cyclohexane at 35 °C for 1 h and drying with a clean air stream.

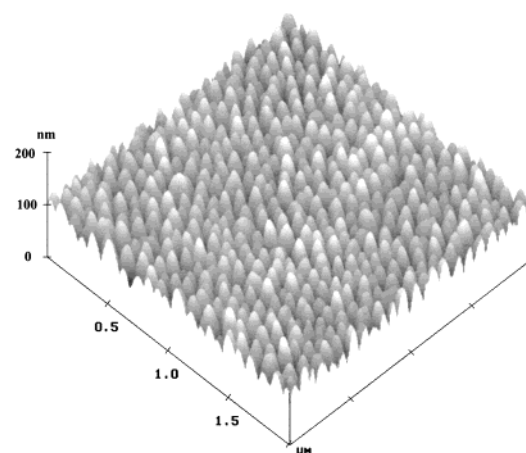


**Figure 3.** AFM image of the tethered PS-*b*-PMMA brushes with 23 nm thick PS layer and 14 nm thick PMMA layer after treatment with a procedure described in ref 31.

makes a contribution to the contact angle;<sup>32</sup> this result is consistent with the prediction that surface roughness increases contact angles larger than 90°. It is unclear what scale of surface roughness affects the contact angle.<sup>32</sup> Our experiments indicate that the surface roughness in AFM image 1 and 2 does not significantly affect the advancing contact angles. XPS results on a nanopattern formed from a PS-*b*-PMMA brush with 26 nm PS layer and 16 nm PMMA layer indicate that the contents of C and O atoms are 95.2 and 4.8%, respectively. These results are consistent with our speculation that PS blocks form a layer around the PMMA core. At this time,  $M_n$ ,  $M_w/M_n$  of PS-*b*-PMMA, and the initiation efficiency of the PMMA-blocks are not known. A detailed investigation of the morphological changes in the ellipsoids with different chemical environments and compositions is under way.

We have speculated that the ellipsoid size is influenced by the block chain lengths; we assume that the block length is proportional to ellipsometric film thickness. In a tethered PS-*b*-PMMA film with 15 nm thick PS and 3 nm thick PMMA, the diameter of the typical ellipsoid is 46 nm after the solvent treatment, and the roughness is 5.27 nm.<sup>33</sup> Although more experiments on controlling ellipsoid size and shape are necessary, the AFM images have demonstrated that the nanopattern scale can be controlled by the block lengths of the brushes.

**Acknowledgment.** This work was financially supported by the Army Research Office (DAAH04-96-1-0018).

**Supporting Information Available:** XPS results and AFM image of PS-*b*-PMMA with 15 nm PS and 3 nm PMMA. (PDF). This material is available free of charge via the Internet at <http://pubs.acs.org>. JA992465Z

(33) See Supporting Information.